Proceedings of the 25th International Conference on
Port and Ocean Engineering under Arctic Conditions
June 9-13, 2019, Delft, The Netherlands

Acoustic emissions as a measure of damage in ice

Ben Lishman[1], Aleksey Marchenko[2], Mark Shortt[3], Peter R Sammonds[3]
[1] School of Engineering, London South Bank University, London, UK
[2] Department of Arctic Technology, University Centre in Svalbard, Longyearbyen, Norway
[3] Institute for Risk and Disaster Reduction, University College London, London, UK

ABSTRACT

When ice is damaged it emits sounds. These sounds can be recorded, and thus may allow us to make direct observations of the way ice breaks. In particular, it would be useful to understand how networks of cracks form in ice after load is applied but before failure occurs. In this work we use new large data sets of acoustic emissions (AE) from saline ice, recorded in the field and in the ice tank, to show how AE records are related to loading patterns. Observations from cyclic loading allow observation of healing processes as well as damage. We show, quantitatively and qualitatively, how AE measurements can help improve understanding of sea ice mechanics.

KEY WORDS: Ice; Fracture; Acoustic Emissions.

INTRODUCTION

One aim of ice mechanics is to develop our understanding of how ice breaks. By understanding failure mechanisms, we can improve predictions of ice forces (which may be limited by the strength of the ice) and basin-scale dynamics (where ice deformation is a significant part of any energy balance). Measurement of acoustic emissions (AE) may help in developing this understanding. Similar measurements have allowed researchers to view crack development over time in rocks and concrete (e.g. Tuffen et al., 2008; Pohoryles et al., 2017), and to develop tools to diagnose material defects (e.g. Elasha et al., 2017).

Acoustic emissions techniques usually rely on recordings of individual 'hits' – short duration (<1ms) pulses of sound which are associated with a single source (e.g. an opening crack). Materials which are experiencing damage can produce thousands of these hits. In many acoustic emissions systems, including those used in this work, each of these hits is recorded as a separate event. Primary features for classifying hits are the amplitude of the hit (i.e. how loud the associated noise was) and the time at which the hit was recorded. Secondary features (which can be derived from analysis of the waveform associated with individual hits) include the

frequency of the sound, and its duration (i.e. how long its RMS amplitude remains above a given threshold).

One way to interpret acoustic emissions is by considering the ratios of relatively loud hits to relatively quiet hits. This can be quantified by plotting the cumulative magnitude distribution of all recorded hits (i.e. the number of recorded hits greater than each amplitude). The slope of this cumulative magnitude distribution is known in the literature as the b-value. If b-values are significantly greater than 1, this means that the material is emitting low-amplitude sounds more often than it is emitting high-amplitude sounds. Typically we might interpret this as the development of unconnected microcracks. If b-values are close to 1, then this means that loud emissions are occurring as often as quiet emissions. At this stage, large cracks are opening as well as small cracks. Overall, then, b-values are expected to decrease during sustained loading, as fracture networks develop, and to fall to a value of 1 at or near failure. These patterns are analogous to Gutenberg-Richter laws in seismology, and similar behavior may be seen in any brittle materials with a self-similar distribution of crack lengths (Sammonds et al., 1994). To summarise: by measuring b-values, we can make tentative conclusions about the distribution of crack sizes within the material, and about the evolution towards failure.

As well as understanding the varying crack distribution during loading, it would be useful to differentiate between fracture modes. Following methods developed in civil engineering, Li and Du (2016) compare laboratory tensile tests to three-point bending tests (on fresh ice), and show that tensile failure leads to AE with high frequencies and low rise times, while shear failure leads to AE with lower frequencies and longer rise times. In principle, this method could be used to distinguish between crack modes in more complex loading configurations.

In this paper we show new results from large AE datasets obtained in field experiments and ice tank experiments. AE measurement on ice in the lab is reasonably well developed (see e.g. St Lawrence and Cole, 1982; Weiss and Grasso 1997; Li and Du 2016) but AE measurements taken on natural sea ice in the field are limited (Zaretsky and Chumichev, 1982; Sinha, 1985; Langhorne and Haskell, 1996; Cole and Dempsey, 2004) and we are unaware of any published data on acoustic emissions recorded at intermediate scales in ice tanks. The new results presented in this paper focus on AE measurements beyond the laboratory.

ACOUSTIC EMISSIONS FROM FIELD EXPERIMENTS

A series of experiments were undertaken on natural sea ice in the Vallunden lake, connected to the Van Mijen Fjord, Svalbard, in March 2016. The sea water salinity in the lake is 34-35ppt, and the ice salinity is 4-7ppt. Ice beams are cut from the natural ice using handsaws, and then forces are applied using hydraulic actuators. Further details can be found in Chistyakov et al., 2016. In this work we compare the results from four in situ tests: a tensile test, a shear test, a compression test and an indentation test. Data from the compression test and indentation test are presented and discussed elsewhere (Lishman et al., 2019). Data from the tensile test and shear test are presented and discussed below.

(a)   (b)   (c)
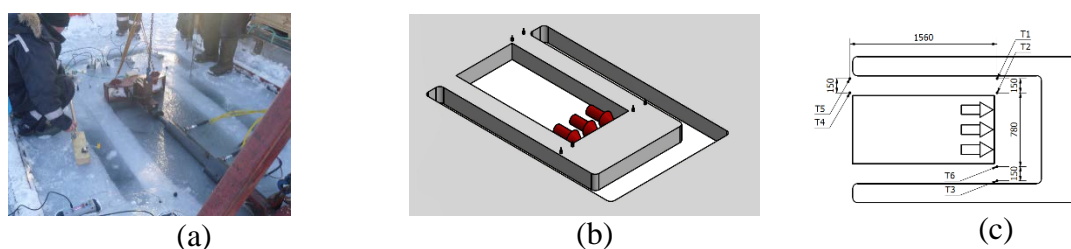
Figure 1: field experiment with ice failure in tension

The tensile test setup is shown in figure 1 (photo (a); simplification (b); detailed layout (c)). Two 'arms' of ice are simultaneously in tension, as the actuator pushes (red arrows) on ice at the end of the arms. Acoustic emissions are recorded on a Vallen AMSY5 bespoke recording system, with PZT-5H compressional crystal sensors (15mm diameter, 5mm thickness). The system has a low frequency cutoff at 100kHz, and we impose a high frequency cutoff at 180kHz to eliminate noise (i.e. the hits shown in this paper all have frequencies between 100kHz and 180kHz). The AE transducers are the black cylinders in figure 1, frozen directly onto the ice surface. Channels 5 and 6 were not recorded, so no data are presented for these tranducers.
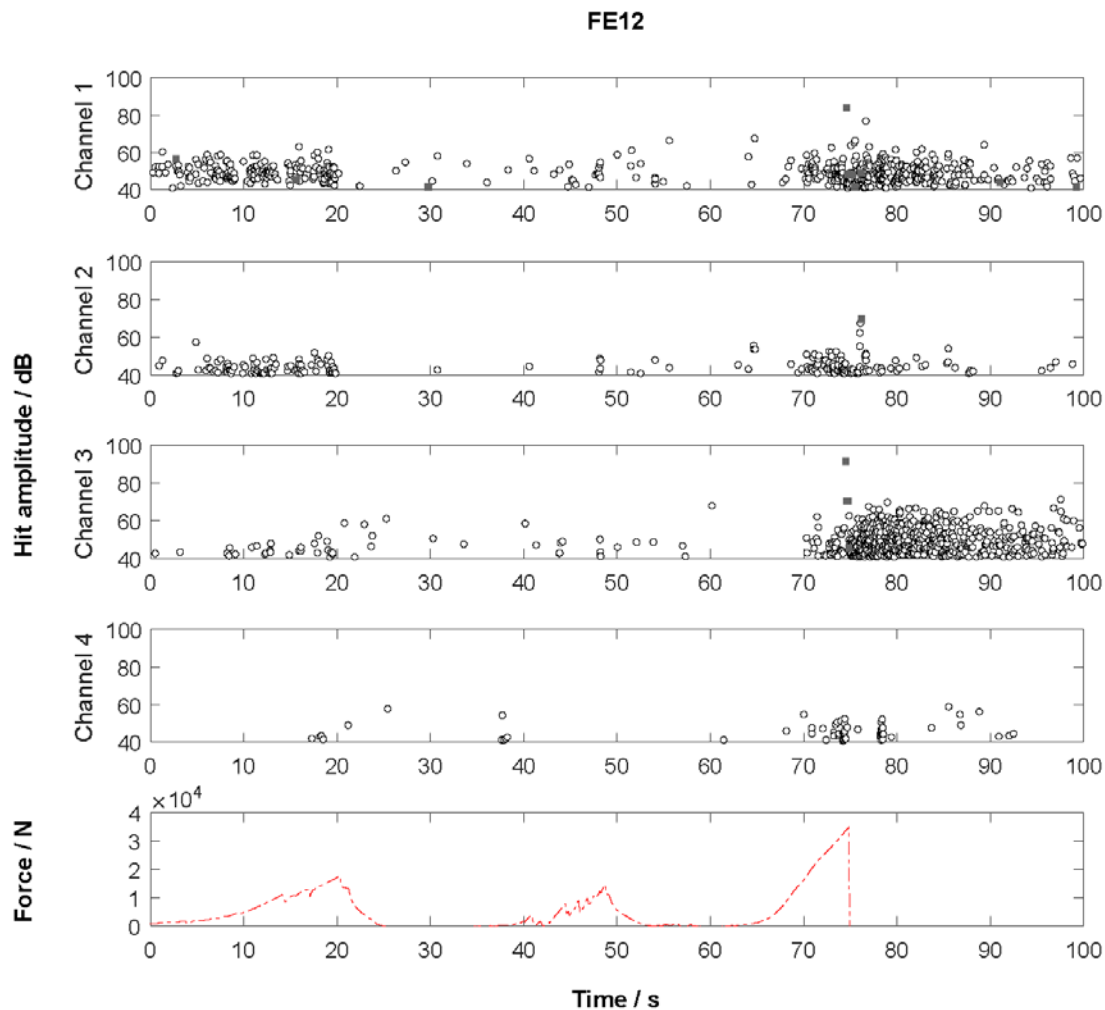
Figure 2: tension experiment hit amplitude and force vs time.

Figure 2 shows the results of the tension test. The upper four plots show hit amplitudes, as a function of time, across four different channels. Circular markers represent hits for which all data was recorded, while square markers represent hits where only an amplitude was recorded (this latter category occurs when the equipment is saturating during periods of high AE – this can be observed on all channels around 74s). The bottom plot shows the force measured at the hydraulic actuator as a function of time. The load was applied twice at low levels to test alignment (~0-20s; ~40-50s) and then applied to failure (~60-75s). Synchronisation between AE plots and load plots is only accurate to ±2s (by direct human communication of when the load was applied). This poor accuracy of load/AE synchronization is a weakness of these experiments, and should be improved in further work. Nevertheless, some features can be noted. AE is visible on each channel and varies between channels. AE appears to be correlated with

loading – increased AE levels are observed from 0-20s; 40-50s; and from around 70s. There are residual high AE levels on channels 1 and 3 after failure (t>74s): these might represent relaxation, or frictional sliding at the broken interface (similar elevated AE levels after failure are seen in rock mechanics experiments (Sammonds et al., 1994)). These correlations between AE and load, and elevated levels of AE after failure, can be seen again in figure 3, which shows hit counts (i.e. hits per second) on each of the four channels during the experiment.
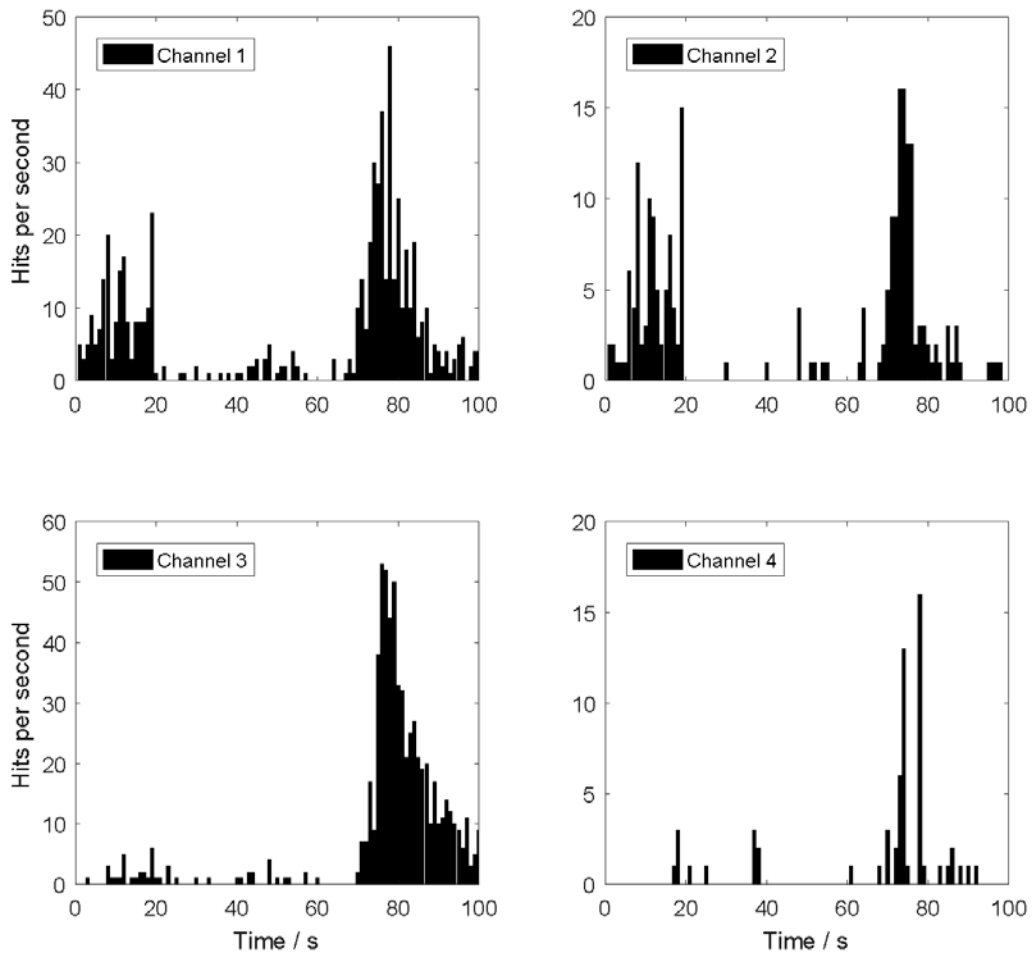
Figure 3: hits per second, recorded on each channel, during the tension experiment.

A second experiment, designed to cause shear failure in the ice, is shown in figure 4 (photo (a); simplification (b); detailed layout (c)). In this experiment, three transducers are deployed, as shown.

(a)   (b)   (c)
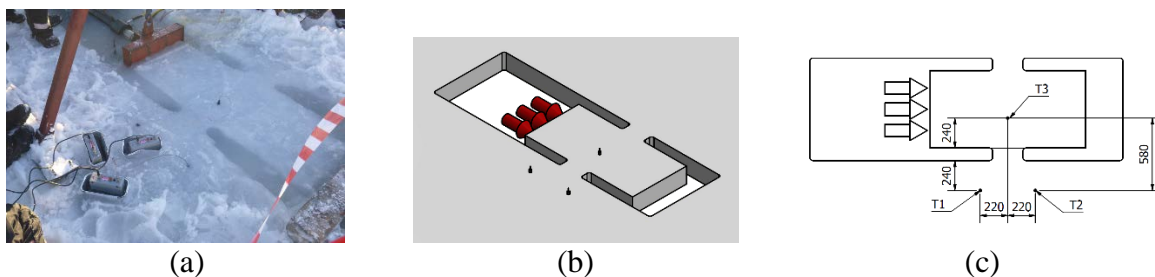
Figure 4: field experiment with ice failure in shear

Results associated with the test in figure 4 are shown in figure 5.
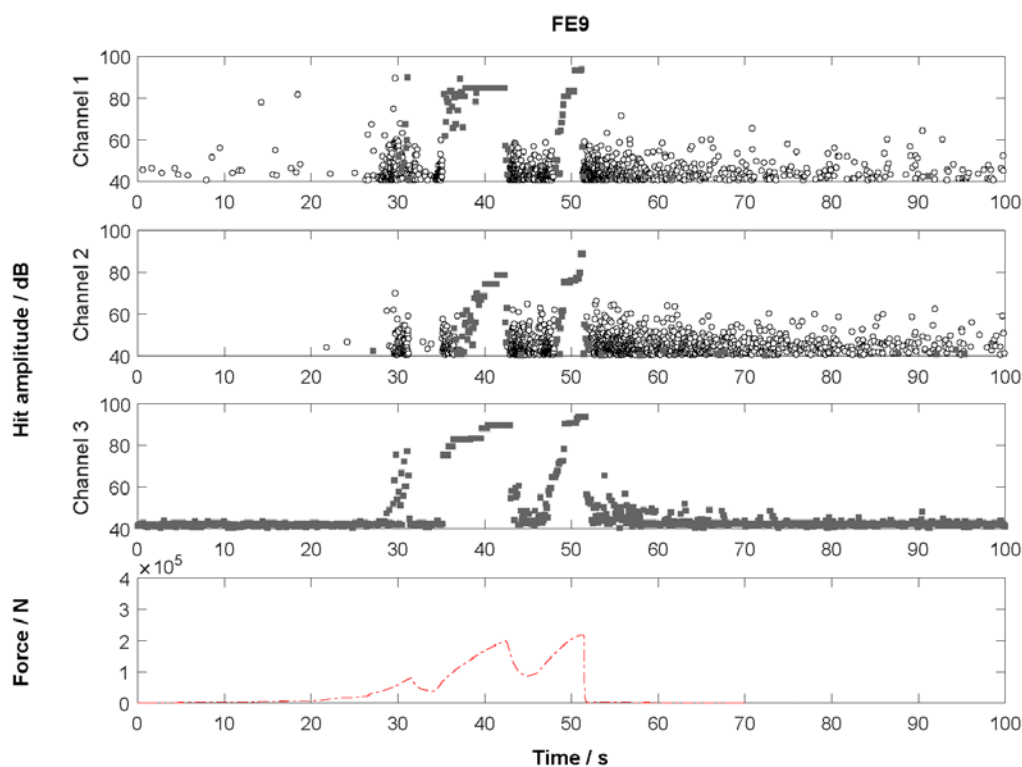
Figure 5: shear experiment hit amplitude and force vs time.

Again, hit amplitudes as a function of time are shown in the upper plots, and force as a function of time is shown in the bottom plot. Here, again, the force is applied in phases, with separate peaks around 32s, 42s and failure around 52s. These peaks can be seen reasonably clearly in each of the AE plots. Again, filled square markers represent data points where the equipment was saturated, and only the maximum values of hits are recorded during these periods of saturation. Again, synchronization between the upper three plots and the bottom plot is ±2s. Again, AE is visible on each channel, is correlated with loading, and remains elevated after failure.

Using the data from the experiments shown in figures 1 and 4, along with data from compression and indentation experiments discussed elsewhere, and following the methodology of Li and Du (2016), we can plot a graph of AF (frequency of the detected sound wave) vs RA (rise time, in seconds, divided by amplitude, in V) for each of the different failure modes. This data is plotted in figure 6. We see no clear pattern here, and this data would not allow us to distinguish between failure modes, i.e. we aren't able to verify the results of Li and Du for in situ natural ice. This is probably because our experiments have a low frequency cutoff at 100kHz, and shear cracks in Li and Du's analysis emit at frequencies around 10kHz. Nevertheless we feel that further analysis and data collection would be beneficial here. In practice, every apparatus will have some low frequency cutoff, and it would be useful to standardize our understanding and our use of equipment so that crack classification can be included in future studies.
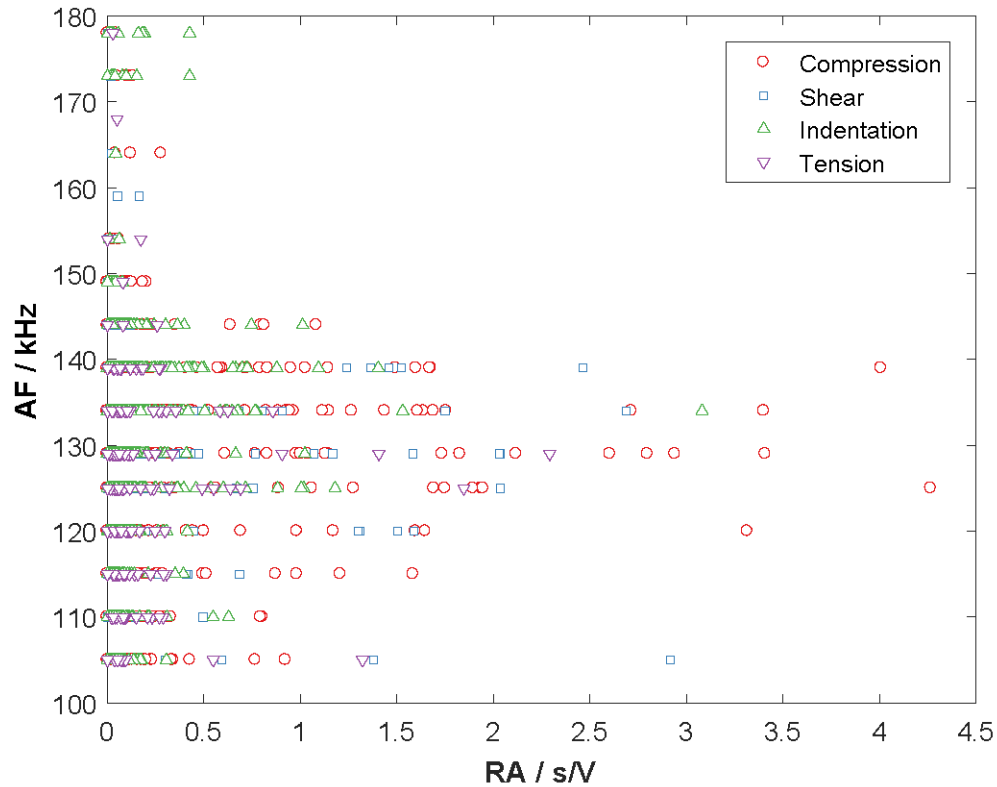
Figure 6: AF vs RA for four experiments: compression (red circles), shear (blue squares), indentation (green triangles) and tension (purple triangles).

ACOUSTIC EMISSIONS FROM ICE TANK EXPERIMENTS

A series of experiments on waves under ice was undertaken in the Large Ice Model Basin of the HSVA ice tank in January 2018. A wave-maker was used to generate waves which passed under a 50m x 10m floating ice sheet. For the experiments described here, the ice sheet was 5cm thick. In each experiment the wave maker was activated for ten minutes, then stopped. The results presented here were recorded on a single AE transducer, 8m from the edge of the ice closest to the wave maker. Further details of the experimental programme can be found in Marchenko et al., 2019.

The results presented in this work are from two tests with identical external conditions, repeated one after the other. In both tests, the wavemaker was set to produce waves at 0.7Hz with open water wave heights of 1cm. The first test ran from approximately 16.20 to 16.30 on the 17th January 2018; the second test ran from approximately 16.40 to 16.50. In other words, each test was ten minutes long, and the gap between tests was ten minutes. Here, we'll refer to the first test as "HSVA 1" and the second test as "HSVA 2". The experiment preceding HSVA 1 finished at 15.00, so that before HSVA 1 there was a gap of 80 minutes with undisturbed ice.

Results for HSVA 1 and HSVA 2 are shown in figures 7 and 8. The horizontal axis for all figures is time, in seconds. The top graph on each figure shows hit amplitudes for all hits (each circle represents an individual hit: 7940 hits were recorded in HSVA 1, and 6585 hits were recorded in HSVA 2). The bottom graph on each figure shows b-values, calculated for groups of 500 hits. (Recall from earlier that b-values are the slopes of cumulative magnitude distributions of hit amplitudes, and that higher b-values indicate higher ratios of low-amplitude hits to high-amplitude hits.)
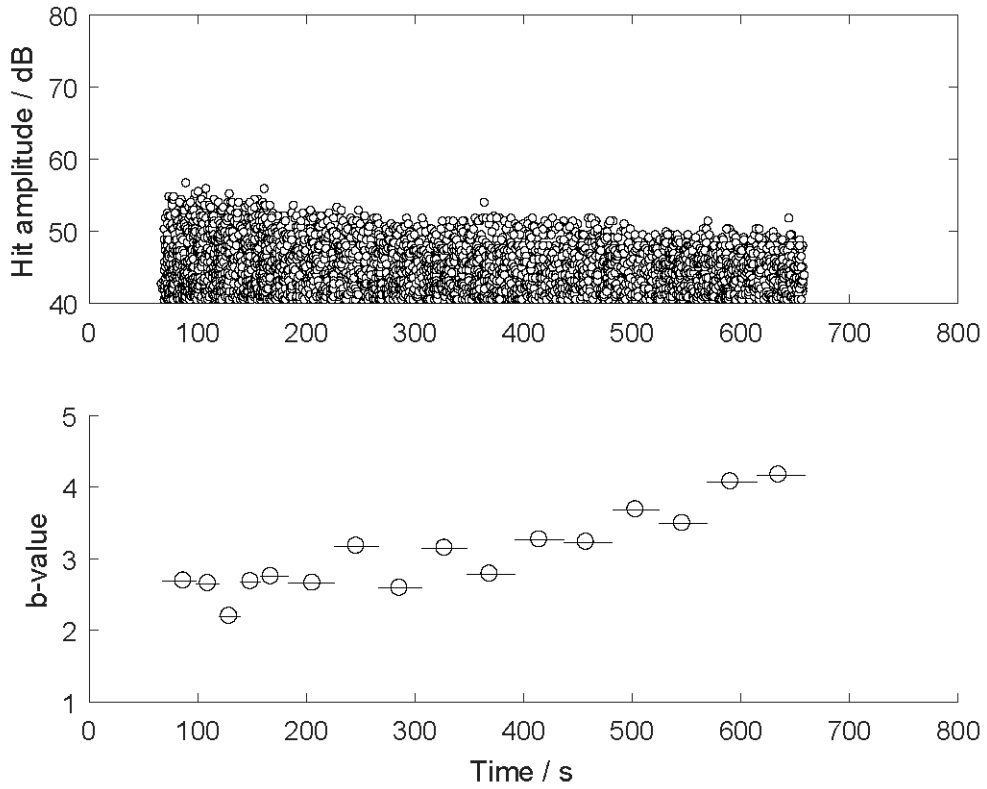
Figure 7: hit amplitudes (top graph) and b-values (bottom graph) vs time for HSVA 1.
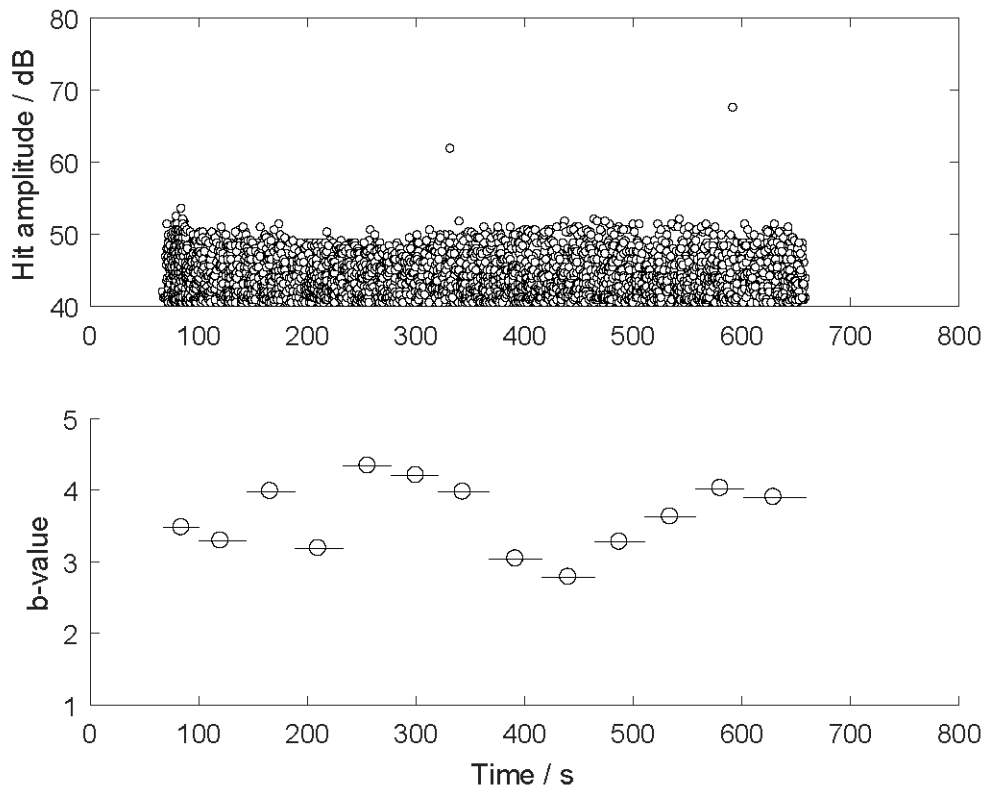
Figure 8: hit amplitudes (top graph) and b-values (bottom graph) vs time for HSVA 2.

Although figures 7 and 8 show results from repetition of a single experiment, the results are somewhat different. Maximum hit amplitudes in HSVA 1 start at around 55dB and decay steadily to around 48dB by the end of the experiment. Maximum hit amplitudes in HSVA 2 start at around 53dB and decay within 20s to around 50dB. b-values for HSVA 1 start below 3, and rise through the experiment to values over 4. b-values in HSVA 2 show a less clear trend, increasing and decreasing throughout the experiment.

The rise in b-values during HSVA 1 suggests that relatively more small cracks, or fewer large cracks, are opening towards the end of the experiment (this corresponds with what we see in the hit amplitude data, where the maximum amplitudes decrease). In HSVA 2, the ratio of small cracks to large cracks varies, with a b-value minimum near the middle of the experiment. In neither case is there any evidence that small cracks are coalescing into larger cracks, as often happens in sustained loading experiments. During wave loading, parts of the ice sheet will go through cycles of compression and tension. It is possible that cracks open during tension and close, and perhaps heal, during compression, so that although new cracks are forming (i.e. we hear AE) the cracks do not form networks and the structure of the ice sheet is undamaged (i.e. the b-values do not decrease and crack amplitudes do not increase). This suggested healing may also be supported by the hit amplitudes at the start of each experiment. In HSVA 1, after 80 minutes of resting/healing, hit amplitudes remain elevated for several hundred seconds, as larger, healed cracks reform while the ice sheet reaches a new dynamic steady state. In HSVA 2, which occurs after 10 minutes of resting/healing, the return to steady state happens more quickly, in around 20s.

CONCLUSIONS

This paper presents acoustic emissions recorded from breaking sea ice in its natural environment and from saline ice deformed by wave action in the HSVA ice tank. In both cases, high numbers (i.e. thousands) of individual acoustic pulses, or hits, in the frequency range 100kHz-180kHz, were recorded during experiments of duration 1-10 minutes, while ice was deforming. In tensile and shear tests of natural sea ice in the field, AE maximum amplitudes were correlated with magnitudes of applied force. Increased numbers of AE hits were observed during periods of high loading. AE hit counts remained elevated after the ice had failed, possibly due to processes associated with relaxation. Within our experimental setup, we are unable to distinguish between shear failure and tensile failure through AF/RA analysis, possible because we are not recording at sufficiently low acoustic frequencies. In experiments in the HSVA ice tank, we record AE from a saline ice sheet deformed by wave action. We record thousands of hits, suggesting that microcracking occurs as the waves pass under the ice. However, b-value analysis suggests that these microcracks do not coalesce into larger cracks: if anything, maximum hit amplitudes decrease during the experiments. We speculate that cracks may be forming and healing repeatedly under cyclic motion. Elevated levels of cracking at the start of experiments, following periods of static healing, support the theory that as well as crack formation, some amount of healing occurs and can be studied by considering patterns of AE.

ACKNOWLEDGEMENTS

REFERENCES

Chistyakov, Karulin, Marchenko, Sakharov, Lishman, 2016. Tensile strength of saline and freshwater ice in field tests. In proc. 23rd IAHR International Symposium on Ice, Ann Arbor, Michigan USA, 31st-3rd June 2016.

Cole, D. M., & Dempsey, J. P. (2004). In situ sea ice experiments in McMurdo Sound: cyclic loading, fracture, and acoustic emissions. Journal of cold regions engineering, 18(4), 155-174.

Elasha, Faris, Matthew Greaves, David Mba, and Duan Fang. "A comparative study of the effectiveness of vibration and acoustic emission in diagnosing a defective bearing in a planetry gearbox." *Applied Acoustics* 115 (2017): 181-195.

Langhorne, P. J., and T. G. Haskell. "Acoustic emission during fatigue experiments on first year sea ice." Cold regions science and technology 24, no. 3 (1996): 237-250.

Li, Dongsheng, and Fangzhu Du. "Monitoring and evaluating the failure behavior of ice structure using the acoustic emission technique." Cold Regions Science and Technology 129 (2016): 51-59.

Lishman, Ben, A. Marchenko, P. Sammonds, A. Murdza, 2019. Acoustic emissions from in situ experiments on field ice. In preparation.

Marchenko, Aleksey, Andrea Haase, Atle Jensen, Ben Lishman, Jean Rabault, Karl-Ulrich Evers, Mark Shortt, and Torsten Thiel. "Laboratory investigations of the bending rheology of floating saline ice, and physical mechanisms of wave damping, in the HSVA ice tank." (in review) arXiv preprint arXiv:1901.05333 (2019).

Pohoryles, Daniel A., Jose Melo, Tiziana Rossetto, Matthias Fabian, Colum McCague, Katerina Stavrianaki, Ben Lishman, and Ben Sargeant. "Use of DIC and AE for monitoring effective strain and debonding in FRP and FRCM-retrofitted RC beams." *Journal of Composites for Construction* 21, no. 1 (2017): 04016057.

Sammonds, Peter R., P. G. Meredith, S. A. F. Murrell, and I. G. Main. "Modelling the damage evolution in rock containing pore fluid by acoustic emission." In Rock Mechanics in Petroleum Engineering. Society of Petroleum Engineers, 1994.

Sinha, 1985, Acoustic emission study on multi-year sea ice in an Arctic field laboratory. J. Acoust. Emission, 4 (2/3) (1985), pp. S290-S293

St Lawrence, William F., and David M. Cole. Acoustic emissions from polycrystalline ice. No. CRREL-82-21. Cold Regions Research and Engineering Lab. Hanover NH, 1982.

Tuffen, Hugh, Rosanna Smith, and Peter R. Sammonds. "Evidence for seismogenic fracture of silicic magma." *Nature* 453, no. 7194 (2008): 511.

Weiss, Jerome, and Jean-Robert Grasso. "Acoustic emission in single crystals of ice." The Journal of Physical Chemistry B 101, no. 32 (1997): 6113-6117.

Zaretsky Y.K., Chumichev B.D.,Short-term creep of ice, Novosibirsk 1982.